PHYSICAL REVIEW B **90**, 180404(R) (2014)

Magnetic-ion-induced displacive electric polarization in FeO_5 bipyramidal units of $(Ba,Sr)Fe_{12}O_{19}$ hexaferrites

Shi-Peng Shen, Yi-Sheng Chai,* Jun-Zhuang Cong, Pei-Jie Sun, Jun Lu, Li-Qin Yan, Shou-Guo Wang, and Young Sun†
Beijing National Laboratory for Condensed Matter Physics, Institute of Physics, Chinese Academy of Sciences, Beijing 100190, China
(Received 2 March 2014; revised manuscript received 3 November 2014; published 18 November 2014)

Electric polarization in conventional paraelectric/ferroelectric oxides usually involves the displacement of nonmagnetic transition-metal ions with an empty d shell. Here we unravel an unusual mechanism for electric polarization based on the displacement of magnetic Fe^{3+} ($3d^5$) ions. Our simulations suggest that the competition between the long-range Coulomb interaction and short-range Pauli repulsion in a FeO_5 bipyramidal unit with proper lattice parameters would favor an off-center displacement of Fe^{3+}, which directly induces a local electric dipole. As a prototype example, we show that the electric dipole of a FeO_5 bipyramid in $(Ba,Sr)Fe_{12}O_{19}$ hexaferrites leads to a different family of magnetic quantum paraelectrics. The manipulation of this unique magnetic-ion-induced displacive electric polarization in a FeO_5 bipyramid could open up a promising route to generating unconventional dielectrics, ferroelectrics, and multiferroics.

DOI: 10.1103/PhysRevB.90.180404 PACS number(s): 77.22.−d, 75.50.Gg, 77.90.+k

In conventional paraelectric and ferroelectric oxides such as perovskite $SrTiO_3$ and $BaTiO_3$, the local electric dipole usually requires an off-center shifting of transition-metal ions with an empty d shell due to the hybridization between the empty d orbital and filled O $2p$ orbitals [1,2]. This empirical "d^0-ness" rule [3] has severely restrained the simultaneous presence of both dielectric and magnetic orders because magnetism normally requires non-d^0 configurations [4]. In order to incorporate paraelectricity/ferroelectricity with magnetism, one has to introduce them independently at different sites [5,6] or by employing other unconventional mechanisms of electric polarization such as noncollinear spin configurations [7], charge ordering [8,9], geometric ferroelectricity [10], etc.

The search for unusual examples that break the empirical d^0-ness rule has been ongoing for a long time, but with little success. Important progress has been made only recently on perovskite manganites. Several first-principle calculations predicted electric polarization in $AMnO_3$ (A = Sr, Ca, and Ba) perovskites driven by the displacement of a magnetic Mn^{4+} ion in a MnO_6 octahedron [11–13]. Soon after, this prediction was experimentally confirmed in $Sr_{1-x}Ba_xMnO_3$ ($x \geqslant 0.45$) crystals [14]. In this Rapid Communication, we demonstrate another intriguing case violating the d^0-ness rule, which is structurally and physically distinct from perovskite oxides. It is found that the delicate balance between the long-range Coulomb interaction and short-range Pauli repulsion in the FeO_5 bipyramid unit with proper lattice parameters would favor an off-center displacement of magnetic Fe^{3+} ions, which directly induces a local electric dipole.

The concept unraveled in this work originates from the understanding of the abnormal dielectric behaviors in $(Ba,Sr)Fe_{12}O_{19}$ hexaferrites. Hexaferrites are iron oxides with hexagonal structures. Depending on their chemical formula and crystal structures, hexaferrites can be classified into several types [15,16]: M-type $(Ba,Sr)Fe_{12}O_{19}$, Y-type $(Ba,Sr)_2Me_2Fe_{12}O_{22}$, W-type $(Ba,Sr)Me_2Fe_{16}O_{27}$, X-type $(Ba,Sr)_2Me_2Fe_{28}O_{46}$, Z-type $(Ba,Sr)_3Me_2Fe_{24}O_{41}$, and U-type $(Ba,Sr)_4Me_2Fe_{36}O_{60}$, where Me is a bivalent metal ion. As shown in Fig. 1, the structures of hexaferrites can be described by a periodically stacking sequence of three basic building blocks (S, R, and T blocks) along the c axis. The Fe^{3+} ions occupy three different kinds of sites: octahedral, tetrahedral, and bipyramidal sites. In particular, the FeO_5 bipyramids only exist in the middle of R blocks where the equatorial plane of the bipyramid is a mirror plane. Among all the hexaferrites, M-type hexaferrites have the simplest crystal structure, consisting of alternate stacks of S and R blocks along the c axis. Both $BaFe_{12}O_{19}$ and $SrFe_{12}O_{19}$ have a collinear ferrimagnetic ordering along the c axis, with a Néel temperature of ~720 [17] and 737 K [18], respectively. This spin configuration persists down to the lowest temperature without any magnetic transition.

We have prepared single-crystal and polycrystalline samples of various hexaferrites to investigate their dielectric properties. The details of sample preparation and structural and magnetic characterizations are given in the Supplemental Material [19]. The dielectric permittivity was measured using an Agilent 4980A *LCR* meter in a cryogen-free superconducting magnet system (Oxford Instruments, TeslatronPT). Magnetic properties were measured in a Quantum Design superconducting quantum interference device. The specific heat measurement was performed in a Quantum Design physical properties measurement system.

As shown in Fig. 2(a), the c-axis dielectric permittivity $\varepsilon_c(T)$ of $BaFe_{12}O_{19}$ increases steadily with decreasing temperature and remains constant below ~5.5 K. This dielectric saturation behavior closely resembles that of quantum paraelectrics such as $SrTiO_3$ [20], $CaTiO_3$ [21], and $KTaO_3$ [22], where the onset of long-range electric order is suppressed by quantum fluctuations. For quantum paraelectrics, the $\varepsilon(T)$ in the entire temperature region can be described by the Barrett formula [23],

$$\varepsilon = \varepsilon_0 + \frac{M}{\left(\frac{1}{2}T_1\right)\coth\left(\frac{T_1}{2T}\right) - T_0}, \quad (1)$$

*yschai@iphy.ac.cn
†youngsun@iphy.ac.cn

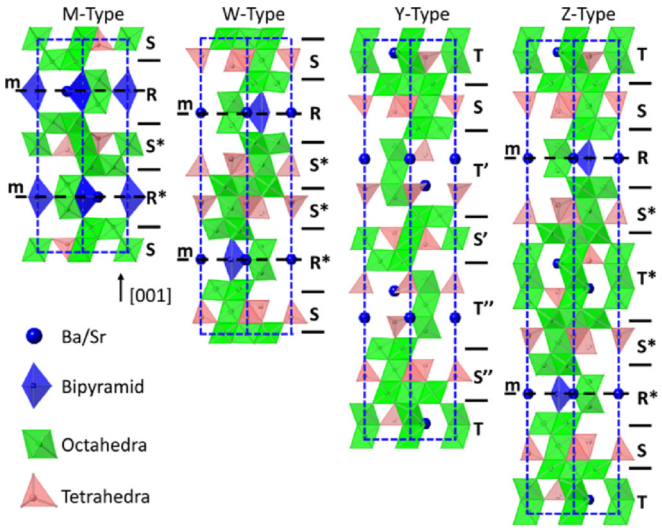

FIG. 1. (Color online) Crystal structures of M-, Y-, W-, and Z-type hexaferrites.

where ε_0 is a constant, T_0 is proportional to the effective dipole-dipole coupling constant, and the positive and negative values correspond to ferro- and antiferroelectric interactions, respectively. T_1 represents the tunneling integral and is a dividing temperature between the low temperature region, where quantum fluctuation is important, and the high temperature region, where the quantum effect is negligible. $M = n\mu^2/k_B$, where n is the density of dipoles and μ denotes the local dipolar moment.

We find that the $\varepsilon_c(T)$ of $BaFe_{12}O_{19}$ can be well fitted by Eq. (1) in the entire temperature region. The parameters obtained from the fitting curve are listed in Table I. The negative value of $T_0 = -11.7$ K implies an antiferroelectric coupling between electric dipoles. The value of $T_1 = 54.9$ K is comparable to that of $SrTiO_3$, but $M = 452$ K is two orders

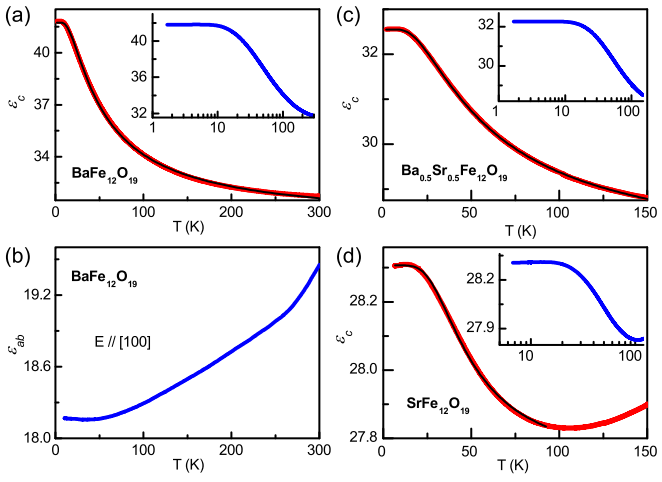

FIG. 2. (Color online) The c-axis dielectric permittivity ε_c at 1 MHz as a function of temperature for (a) $BaFe_{12}O_{19}$, (c) $Ba_{0.5}Sr_{0.5}Fe_{12}O_{19}$, and (d) $SrFe_{12}O_{19}$. (b) The ab-plane dielectric permittivity ε_{ab} for $BaFe_{12}O_{19}$. The black solid lines are the fitting curves to Eq. (1). The insets are the same plots with a logarithmic scale in temperature.

TABLE I. The fitting parameters T_0, T_1, and M to Eq. (1). The values in bold are unreliable. The Fe-O bond lengths in the FeO_5 bipyramid for $BaFe_{12}O_{19}$ and $SrFe_{12}O_{19}$ at room temperature are derived from Ref. [30]. The bond lengths of $Ba_{0.5}Sr_{0.5}Fe_{12}O_{19}$ are linearly extrapolated from those of the end members.

$Ba_{1-x}Sr_xFe_{12}O_{19}$	$x = 0.0$	$x = 0.5$	$x = 1.0$
T_0 (K)	-11.7 ± 0.2	-9.7 ± 0.2	**53.1** $\pm$ 0.3
T_1 (K)	54.9 ± 0.2	67.6 ± 0.2	**130.6** $\pm$ 0.5
M (K)	452 ± 1.6	224.4 ± 0.8	7.4 ± 0.1
Fe-O_{ap} (Å)	2.33	2.32	2.31
Fe-O_{ab} (Å)	1.87	1.865	1.86

of magnitude smaller than that of $SrTiO_3$. We note that this quantum paraelectric behavior is observable only along the c axis. As shown in Fig. 2(b) for comparison, the ab-plane dielectric permittivity measured along the [100] direction decreases monotonically with decreasing temperature, which suggests that the electric dipoles in $BaFe_{12}O_{19}$ are along the c axis. To further verify that the saturation of ε_c at low temperatures has nothing to do with any phase transition, we measured the specific heat C_P of $BaFe_{12}O_{19}$ down to 2 K. No anomaly due to a phase transition could be detected (see the Supplemental Material [19]). Therefore, $BaFe_{12}O_{19}$ is a distinctive quantum paraelectric with a hexagonal structure, in contrast to well-known perovskite quantum paraelectrics.

Similarly, isostructural $Ba_{0.5}Sr_{0.5}Fe_{12}O_{19}$ and $SrFe_{12}O_{19}$ also exhibit quantum paraelectric behavior, as shown in Figs. 2(c) and 2(d). The fitting curve of Eq. (1) for $Ba_{0.5}Sr_{0.5}Fe_{12}O_{19}$ gives smaller parameters for both T_0 and M, indicating a weaker dipole-dipole coupling and a smaller local dipole moment than $BaFe_{12}O_{19}$. Note that there is a relatively larger $\varepsilon_c(T)$ background above 100 K in $SrFe_{12}O_{19}$ due to the rise of conductivity at high temperatures. Therefore, the fitting parameters of T_0 and T_1 for $SrFe_{12}O_{19}$ are not reliable while the parameter M is not so sensitive to the high temperature background that it does not lose its physical meaning. The decreasing parameter M suggests that the local dipole moment decreases with Sr content. Since the discovery of quantum paraelectricity in $SrTiO_3$ [20], magnetic quantum paraelectrics where quantum paraelectricity coexists with magnetic ordering have been rarely found. The only known example so far is $EuTiO_3$, which exhibits quantum paraelectricity along with an antiferromagnetic order [24]. The (Ba,Sr)$Fe_{12}O_{19}$ hexaferrites represent a different family of ferrimagnetic quantum paraelectrics with magnetodielectric effects (see the Supplemental Material [19]).

The quantum paraelectric behaviors in (Ba,Sr)$Fe_{12}O_{19}$ reveal the existence of local electric dipoles whose origin must be related to magnetic Fe^{3+} ions. As seen in Fig. 1, the structure of (Ba,Sr)$Fe_{12}O_{19}$ consists of alternating R and S blocks. The FeO_5 bipyramids residing in the middle of the R blocks, if in the centrosymmetric structure with space group $P6_3/mmc$, would not generate local electric dipoles. However, some experiments [25,26] have suggested the existence of off-equatorial displacements of Fe^{3+} at a Wyckoff position of the 2b site, which results in two adjacent Wyckoff positions of 4e sites with a lowered symmetry. If the off-equatorial

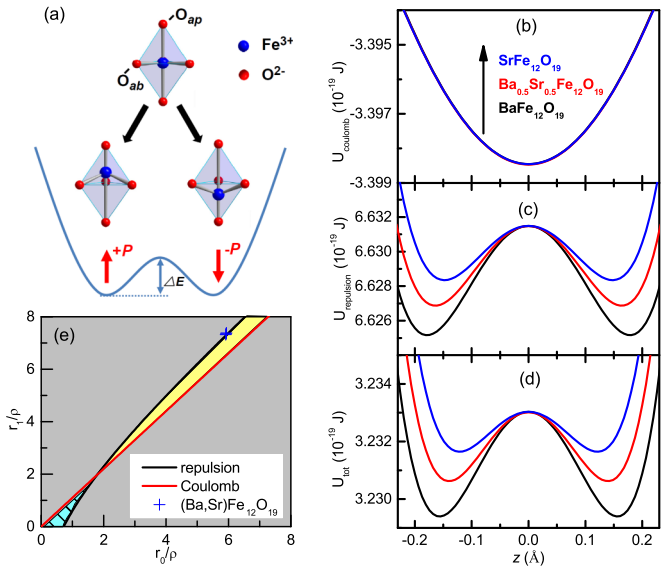

FIG. 3. (Color online) (a) Schematic illustration of Fe^{3+} off-equatorial displacements in the FeO_5 bipyramid. The up and down displacements correspond to two $4e$ sites with opposite dipoles and local minima in the energy potential. The calculated energy potentials from Eq. (2) for (b) U_{Coulomb}, (c) $U_{\text{repulsion}}$, and (d) the sum U_{tot} as a function of off-equatorial Fe^{3+} displacement z in $(Ba,Sr)Fe_{12}O_{19}$. (e) Phase diagram to allow the double-well potential. In the central yellow region, the double-well potential is not allowed. In the left corner (blue), it must appear. In the rest regions (gray), it is possible due to the competition between the Coulomb attraction and Pauli repulsion.

displaced Fe^{3+} at the $4e$ sites has a lower energy than the highly symmetric $2b$ sites, a local electric dipole P along the c axis would be favored, as illustrated in Fig. 3(a). From the fitted M values and the nominal density of $4e$ sites, $n = 2.86 \times 10^{27}\,\text{m}^{-3}$, the local dipole moments $\mu = 0.68$, 0.50, and 0.09 e Å are obtained for $BaFe_{12}O_{19}$, $Ba_{0.5}Sr_{0.5}Fe_{12}O_{19}$, and $SrFe_{12}O_{19}$, respectively. The decreasing dipole moment with increasing Sr content suggests smaller off-equatorial displacements for the $4e$ sites, which is consistent with the x-ray refinement results [25,27] where the $4e$-$4e$ distance at room temperature decreases from 0.34(1) to 0.194(10) Å from $BaFe_{12}O_{19}$ to $SrFe_{12}O_{19}$. A Mössbauer study [28] also revealed a similar tendency at 4.2 K, where the $4e$-$4e$ distances are 0.176(5) and 0.133 for $BaFe_{12}O_{19}$ and $SrFe_{12}O_{19}$, respectively.

To give a more convincing assessment of the origin of the local dipoles, we performed theoretical simulations on the local potential energy profiles along the c axis within the FeO_5 bipyramid for $(Ba,Sr)Fe_{12}O_{19}$. We adopted a phenomenological local potential energy of the following form for the bipyramid [29],

$$\begin{aligned} U_{\text{tot}}(z) &= U_{\text{Coulomb}}(z) + U_{\text{repulsion}}(z) \\ &= -\frac{3\times 6e^2}{\sqrt{r_0^2+z^2}} - \frac{6e^2}{r_1+z} - \frac{6e^2}{r_1-z} \\ &\quad + 3\beta c_{+-} e^{(r_+ + r_- - \sqrt{r_0^2+z^2})/\rho} + \beta c_{+-} e^{[r_+ + r_- - (r_1+z)]/\rho} \\ &\quad + \beta c_{+-} e^{[r_+ + r_- - (r_1-z)]/\rho}, \end{aligned} \tag{2}$$

where z is the c-axis Fe^{3+} displacement away from the $2b$ site. The sum of the first three terms corresponds to the Coulomb potential U_{Coulomb} between Fe^{3+} and O^{2-} and the sum of the remaining the three terms represents the short-range Pauli repulsion potential $U_{\text{repulsion}}$. $(Ba,Sr)Fe_{12}O_{19}$ is assumed to be a pure ionic crystal that the O ion has a $-2e$ charge and the Fe ion has a $+3e$ charge, where e is the electron charge. r_0 and r_1 are the in-plane and out-of-plane Fe-O distances in the bipyramid for $2b$ sites, obtained from Ref. [30] and Table I. β is a constant (taken to be 1.35×10^{-19} J), $c_{+-} = 1$ is Pauling's valence factor, and $\rho = 0.315$ Å is a parameter derived from FeO [29]. $r_+ = 1.4$ Å and $r_- = 0.58$ Å are the ionic radii of Fe^{3+} with a coordinate number of 5 and O^{2-} with a coordinate number of 6, respectively, from Ref. [31].

The calculated results are shown in Figs. 3(b)–3(d). Only the $U_{\text{repulsion}}$ terms show the double-well potential feature near $z = 0$ for the parameters we used. The double well in $U_{\text{repulsion}}$ terms becomes smaller and closer with increasing Sr content while the U_{Coulomb} terms are largely invariant near $z = 0$. Their summation U_{tot} remains the double-well feature, indicating the existence of local electric dipoles in $(Ba,Sr)Fe_{12}O_{19}$. In particular, the $4e$-$4e$ distances estimated from the simulation decrease systematically from 0.310 to 0.245 Å by substituting Ba with Sr, which is consistent with the decreasing tendency of local dipoles by Sr doping found in our experiments. Based on the above calculations, the short-range Pauli repulsions instead of the Coulomb forces favor the off-equatorial arrangement of the Fe^{3+} ion. This is in marked contrast to the case in ABO_3 perovskite ferroelectrics where the long-range Coulomb forces favor the ferroelectric state and short-range repulsions do not. It is very likely due to the unique FeO_5 bipyramid structure as well as the half-filled configuration of Fe^{3+} ($3d^5$). We note that a recent first-principles calculation on $BaFe_{12}O_{19}$ predicted a frustrated antiferroelectric ground state below 3 K associated with its bipyramidal $4e$ sites [32]. On the contrary, in experiments we did not observe any trace of long-range ordering down to 1.5 K, which indicates that the theoretical calculation could have either ignored the quantum tunneling effect or overestimated the dipole-dipole coupling in $BaFe_{12}O_{19}$.

To provide further insight for the lattice requirements to enable local electric dipoles in the FeO_5 bipyramid, we analyzed the extreme conditions of each potential function at $z = 0$. For the Coulomb term to favor off-center displacement of the Fe^{3+} ion it should have $\partial^2 U_{\text{Coulomb}}/\partial z^2|_{z=0} < 0$. One can obtain the corresponding structure requirement, $r_1/r_0 < (4/3)^{1/3} \approx 1.1$. This condition is always unsatisfied for $(Ba,Sr)Fe_{12}O_{19}$ since $r_1/r_0 > 1.23$ for all the members. For the repulsion term to have the double-well feature it should have $\partial^2 U_{\text{repulsion}}/\partial z^2|_{z=0} < 0$. One then obtains the lattice criteria, $e^{r_1/\rho} > 2/3(r_0/\rho e^{r_0/\rho})$. The satisfaction of this criterion depends on the relative magnitude of r_1 and r_0 to ρ, and it happens to be the case for $(Ba,Sr)Fe_{12}O_{19}$. By combining the conditions of both potential terms, we obtained the phase diagram in the r_1/ρ vs r_0/ρ plot, as shown in Fig. 3(e). $(Ba,Sr)Fe_{12}O_{19}$ are found to lie just outside the nonpolar region.

If the local dipoles are really related to FeO_5 bipyramids within the R blocks, one may expect a similar dielectric behavior in other hexaferrites containing the R blocks. To

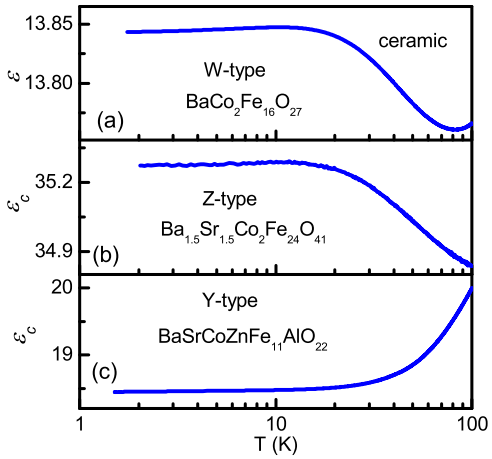

FIG. 4. (Color online) The temperature dependent dielectric permittivity at 1 MHz of (a) the W-type hexaferrite $BaCo_2Fe_{16}O_{27}$ ceramic, (b) the Z-type hexaferrite $Ba_{1.5}Sr_{1.5}Co_2Fe_{24}O_{41}$ single crystal along the c axis, and (c) the Y-type hexaferrite $BaSrCoZnFe_{11}AlO_{22}$ single crystal along the c axis.

clarify this point, we further studied a series of available hexaferrites, including Y-type ($BaSrCoZnFe_{11}AlO_{22}$) and Z-type ($Ba_{1.5}Sr_{1.5}Co_2Fe_{24}O_{41}$) single crystals, and W-type ($BaCo_2Fe_{16}O_{27}$) ceramics. For Y- and Z-type hexaferrites, a constant in-plane magnetic field of 5 kOe is applied to stabilize the transverse cone spin configuration below 150 K during the measurements [33,34]. As shown in Figs. 4(a) and 4(b), the W- and Z-type hexaferrites that contain the R blocks indeed show a sign of quantum paraelectricity, with a similar saturating behavior to that in $(Ba,Sr)Fe_{12}O_{19}$. In strong contrast, the Y-type hexaferrite does not show such a saturation behavior. This is exactly consistent with our expectation because Y-type hexaferrites do not contain FeO_5 bipyramids.

Based on the above experiments and theoretical calculations, we have disclosed a mechanism of electric polarization based on the FeO_5 bipyramid. This unique magnetic-ion-induced displacive polarization, against the "d^0-ness" rule, provides a different resource for generating a variety of exotic dielectric materials. The magnetic quantum paraelectrics of $(Ba,Sr)Fe_{12}O_{19}$ is just one good example. In principle, the amplitude of the electric dipoles and the coupling between them can be enhanced by manipulating the lattice parameters as well as the density of the bipyramid units by pressure, strain, or chemical engineering, which may eventually yield long-range electric orders and multiferroics in bulk crystals or thin films. In terms of the general concept unraveled in this work, unconventional ferroelectrics and multiferroics may be found in a wide range of compounds containing FeO_5 bipyramids, such as $BaFe_4M_2O_{11}$ (M = Sn, Ti, Mn), hexagonal $RFeO_3$ (R = Y, In, Eu − Lu), and many others.

This work was supported by the Natural Science Foundation of China (Grants No. 11227405 and No. 11374347), the National Key Basic Research Program of China (Grant No. 2011CB921801), and the Strategic Priority Research Program of the Chinese Academy of Sciences (Grant No. XDB07030200).

[1] R. E. Cohen, Nature (London) **358**, 136 (1992).
[2] R. E. Cohen and H. Krakauer, Ferroelectrics **136**, 65 (1992).
[3] B. T. Matthias, Phys. Rev. **75**, 1771 (1949).
[4] N. A. Hill, J. Phys. Chem. B **104**, 6694 (2000).
[5] R. Seshadri and N. A. Hill, Chem. Mater. **13**, 2892 (2001).
[6] W. Wang, L.-Q. Yan, J.-Z. Cong, Y.-L. Zhao, F. Wang, S.-P. Shen, T. Zou, D. Zhang, S.-G. Wang, X.-F. Han, and Y. Sun, Sci. Rep. **3**, 2024 (2013).
[7] S.-W. Cheong and M. Mostovoy, Nat. Mater. **6**, 13 (2007).
[8] N. Ikeda, H. Ohsumi, K. Ohwada, K. Ishii, T. Inami, K. Kakurai, Y. Murakami, K. Yoshii, S. Mori, Y. Horibe, and H. Kitô, Nature (London) **436**, 1136 (2005).
[9] Y. Sun, L.-Q. Yan, and J.-Z. Cong, Sci. China: Phys., Mech. Astron. **56**, 222 (2013).
[10] B. B. van Aken, T. T. M. Palstra, A. Filippetti, and N. A. Spaldin, Nat. Mater. **3**, 164 (2004).
[11] S. Bhattacharjee, E. Bousquet, and P. Ghosez, Phys. Rev. Lett. **102**, 117602 (2009).
[12] J. M. Rondinelli, A. S. Eidelson, and N. A. Spaldin, Phys. Rev. B **79**, 205119 (2009).
[13] J. H. Lee and K. M. Rabe, Phys. Rev. Lett. **104**, 207204 (2010).
[14] H. Sakai, J. Fujioka, T. Fukuda, D. Okuyama, D. Hashizume, F. Kagawa, H. Nakao, Y. Murakami, T. Arima, A. Q. R. Baron, Y. Naguchi, and Y. Tokura, Phys. Rev. Lett. **107**, 137601 (2011).
[15] P. B. Braun, Phillips Res. Rep. **12**, 491 (1957).
[16] J. A. Kohn, D. W. Eckart, and C. F. Jr Cook, Science **172**, 519 (1971).
[17] J. Smit and H. P. J. Wijn, *Ferrites* (Phillips Technical Library, Eindhoven, 1959).
[18] Z. F. Zi, Y. P. Sun, X. B. Zhu, Z. R. Yang, J. M. Dai, and W. H. Song, J. Magn. Magn. Mater. **320**, 2746 (2008).
[19] See Supplemental Material at http://link.aps.org/supplemental/10.1103/PhysRevB.90.180404 for the details of sample preparation, characterization, heat capacity, and the magnetodielectric effect.
[20] K. A. Müller and H. Burkhard, Phys. Rev. B **19**, 3593 (1979).
[21] V. V. Lemanov, A. V. Sotnikov, and E. P. Smirnova, Solid State Commun. **110**, 611 (1999).
[22] A. R. Akbarzadeh, L. Bellaiche, K. Leung, J. Íñiguez, and D. Vanderbil, Phys. Rev. B **70**, 054103 (2004).
[23] J. H. Barrett, Phys. Rev. **86**, 118 (1952).
[24] T. Katsufuji and H. Takagi, Phys. Rev. B **64**, 054415 (2001).
[25] X. Obradors, A. Collomb, M. Pernet, D. Samaras, and J. C. Joubert, J. Solid State Chem. **56**, 171 (1985).
[26] J. G. Rensen and J. G. van Wieringen, Solid State Commun. **7**, 1139 (1969).
[27] X. Obradors, X. Solans, A. Collomb, D. Samaras, J. Rodriguez, M. Pernet, and M. F.-Altaba, J. Solid State Chem. **72**, 218 (1988).
[28] G. Albanses, A. Deriu, and D. Cabrini, Hyperfine Interact. **70**, 1087 (1992).

[29] S. P. Marshall and J. B. Sokoloff, Phys. Rev. B **44**, 619 (1991).
[30] O. P. Aleshko-Ozhevskii, M. K. Faek, and I. I. Yamzin, Sov. Phys. Crystallogr. **14**, 367 (1969).
[31] R. D. Shannon, Acta Crystallogr., Sect. A **32**, 751 (1976).
[32] P. S. Wang and H. J. Xiang, Phys. Rev. X **4**, 011035 (2014).
[33] S.-P. Shen, L.-Q. Yan, Y.-S. Chai, J.-Z. Cong, and Y. Sun, Appl. Phys. Lett. **104**, 032905 (2014).
[34] M. Soda, T. Ishikura, H. Nakamura, Y. Wakabayashi, and T. Kimura, Phys. Rev. Lett. **106**, 087201 (2011).